CALIBRATION OF WHITE RICE SIMULATION PARAMETERS BASED ON DISCRETE ELEMENT METHOD
/
基于离散元模拟的白米仿真参数标定

Biao XIE, Jinyin BAI, Jiagang YAN, Shibo ZHAO, Nian LIU, Qiang ZHANG*) [1]
College of Engineering, Huazhong Agricultural University, Wuhan / China;
Key Laboratory of Agricultural Equipment in Mid-lower Yangtze River, Ministry of Agriculture, Wuhan / China
Tel: +86 27 87282120; E-mail: zq604@mail.hzau.edu.cn
DOI: https://doi.org/10.35633/inmateh-71-18

Keywords: *white rice, discrete element method, angle of repose, parameter calibration*

ABSTRACT
Aiming at the lack of discrete element simulation models and parameters for rice polishing, grading, color sorting and other technologies and equipment, and the difficulty of guiding equipment design and optimization through simulation, this paper calibrates the simulation parameters of white rice based on angle of repose (AOR) test and simulation methods. Huanghuazhan and Dongnong 429 white rice were selected as research object. Numerical model of white rice was established by multi-sphere filling. According to physical test and references, the simulation parameter range of white rice particles was determined. Plackett-Burman test was used to screen parameters, and it was found that the particle-particle static friction coefficient and particle-particle rolling friction coefficient had significant effects on the AOR of white rice. The regression model between the AOR and the significance parameter was established according to the central composite design method. The simulation parameter combination that has significant influence on the physical AOR was determined through the optimization design, and verified by the simulation test. The simulation AOR was compared with the physical AOR, and the relative error of the two kinds of white rice was less than 3%. The results show that the calibration method proposed in this study can accurately simulate the physical AOR test, which can provide reference for discrete element simulation of white rice processing.

摘要
针对大米加工中抛光、分级和色选等技术和装备缺乏离散元仿真模型和参数，难以通过仿真指导装备设计与优化等问题，本文基于物理堆积试验和仿真方法对白米仿真参数进行标定。以黄华占和东农 429 两种白米为研究对象，采用多球填充建立了白米颗粒离散元数值模型；根据物理试验和参考文献确定了白米颗粒仿真参数范围；利用 Plackett-Burman 试验进行参数筛选，发现颗粒-颗粒静摩擦系数、颗粒-颗粒动摩擦系数对白米堆积角影响显著；并根据中心复合试验设计方法建立了堆积角与显著性参数间的回归模型；通过寻优设计确定对物理堆积角影响显著的仿真参数组合，并进行仿真试验验证，将仿真所得堆积角与物理试验值进行对比验证，两种白米的相对误差均小于 3%。结果表明，该研究提出的标定方法能准确模拟物理堆积试验，可为大米加工离散元仿真提供参考。

INTRODUCTION
Rice is one of the most important food crops in the world. Consumers are often influenced by psychology and perception when buying rice, so they preferentially choose rice with high appearance quality (*Zhao et al., 2023; Lu et al., 2019*). Rice is usually processed into commercial rice by drying, husking, milling, polishing, grading and color sorting (*Riaz et al., 2017*). Polishing, grading and color sorting are rice finishing, which can increase quality of rice and improve the competitiveness of rice products (*Ahmed et al., 2021*). The traditional rice finishing machinery design mainly relies on the processing experience, which is difficult to guide the optimization design of the processing equipment.

Discrete element method (DEM) reveals the motion characteristics and processing characteristics of the material from the particle scale, which has been widely used in agricultural material processing (*Zhao et al., 2021*), but there are few studies on rice finishing equipment by using the DEM. In order to improve the simulation accuracy, a large number of scholars have calibrated the parameters of dry and wet particle (*Zeng et al., 2021*).

[1] *Biao Xie, M.S. Stud. Eng.; Jinyin Bai, M.S. Stud. Eng.; Jiagang Yan, M.S. Stud. Eng.; Shibo Zhao, B.S. Stud. Eng.; Nian Liu, Prof. Ph.D. Eng.; Qiang Zhang, Prof. Ph.D. Eng.*

In this paper, the simulation parameter ranges of white rice were determined based on physical test and references. Taking the angle of repose (AOR) of physical test as the response value, the regression model between the response value and significant simulation parameters was established by Plackett-Burman (PB) test, steepest ascent test and central composite test design, and the white rice simulation parameters were obtained. The reliability of simulation parameters was verified by comparing the simulation AOR under the combination of optimal parameters with the physical AOR, so as to provide accurate and reliable simulation models and parameter calibration methods for rice polishing, grading, color sorting and other mechanized operations, and provide theoretical support for mechanical device design.

MATERIALS AND METHODS

Test materials

Indica Huanghuazhan and japonica Dongnong 429 rice varieties were selected in the test, among which the type of Huanghuazhan was long-grain and the type of Dongnong 429 was short-grain. The white rice for test was obtained by husking, milling and removing the broken rice. The moisture content of Huanghuazhan white rice (HWR) was 11.3%, and that of Dongnong 429 white rice (DWR) was 12.1%. The main materials of rice polishing, grading and color sorting machine were stainless steel. Therefore, the contact material of this research device was stainless steel.

Numerical model construction of white rice particle

One hundred grains of HWR and one hundred grains of DWR were randomly selected, and the triaxial dimensions (L, B, T) of the grains were measured with digital display vernier caliper (accuracy 0.01) (DL91150, Deli Office Technology Co., LTD., Ningbo, China). The Dimensional measurement diagram is shown in Fig. 1. To simplify the simulation model of white rice, white rice could be regarded as an axisymmetric ellipsoid (*Markauskas and Kačianauskas, 2011*). The length L was taken as the long axis D_L of the ellipsoid model, and the average value of the width B and thickness T were taken as the short axis D_S of the ellipsoid, as shown in Equations (1) and (2). In order to more directly reflect the differences between HWR and DWR, sphericity S_p was introduced for comparison (*Liu et al., 2018*). Sphericity (S_p) was calculated as shown in Equation (3). Results are shown in Table 1. Obviously, there was a clear difference in grain shape between the two types of white rice, and DWR possessed a higher S_p.

$$D_L = L \tag{1}$$

$$D_S = \frac{(B+T)}{2} \tag{2}$$

$$S_P = \frac{(LBT)^{\frac{1}{3}}}{L} \tag{3}$$

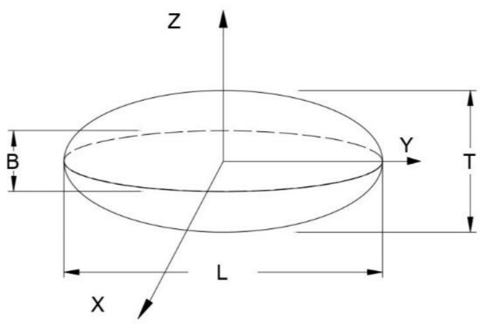

Fig. 1 - Dimensional measurement diagram

According to the simplified ellipsoid sizes of two kinds of white rice, three-dimensional model was established using SolidWorks 2018 (SolidWorks Inc., Concord, USA) software. The 3D model was imported into EDEM 2018 software (DEM Solutions Inc., Edinburgh, Britain) and filled with spheres. The white rice ellipsoid of HWR was filled with 9 spheres, and the white rice ellipsoid of DWR was filled with 7 spheres. The comparison between the discrete element model of white rice and the real rice was shown in Fig. 2, and the discrete element model of rice grain was close to the real shape.

Table 1

Triaxial dimensions and ellipsoid dimensions of white rice

	$L(D_L)$/mm	B/mm	T/mm	D_s/mm	S_p
HWR	6.83±0.26	1.98±0.10	1.70±0.07	1.98±0.08	0.44±0.01
DWR	5.59±0.20	2.61±0.12	1.88±0.10	2.45±0.08	0.54±0.02

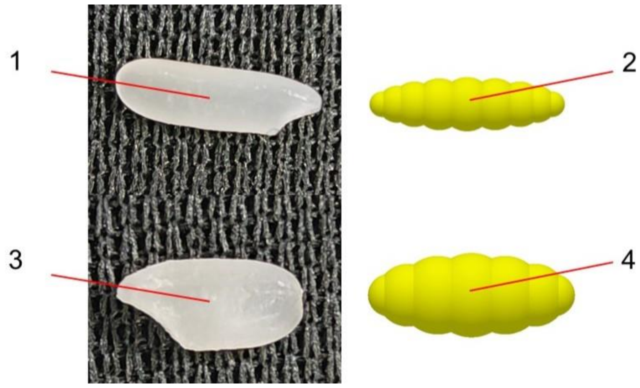

Fig. 2 - Comparison between the discrete element model and the actual condition
1-HWR; 2-model of HWR; 3-DWR; 4-model of DWR

AOR test

The funnel method was used for AOR test of white rice to calibrate the simulation parameters of white rice (*Gong et al., 2021; Liu et al., 2020*). The physical test device was shown in Fig. 3(a), and the simulation test device was shown in Fig. 3(b). The tube length of the funnel was 50 mm, the inner diameter of the funnel outlet was 15 mm, and the distance between the funnel outlet and the stainless steel plate was 50 mm. 40 g white rice was poured into the funnel, and then the discharge port was opened. After white rice was still, the front view was photographed by the camera. Matlab R2018b (The Math Works Inc, Natick, Massachusetts, USA) was used to process the image, as shown in Fig. 4. Binarization, boundary extraction and boundary fitting were carried out in turn, and the slope of the fitting curve was the tangent value of the AOR. The test was repeated for 5 times, and the AOR of the left and right sides of the white rice pile were extracted in each test, and their average values were taken. The physical AOR of HWR was 32.38° and that of DWR was 33.46°.

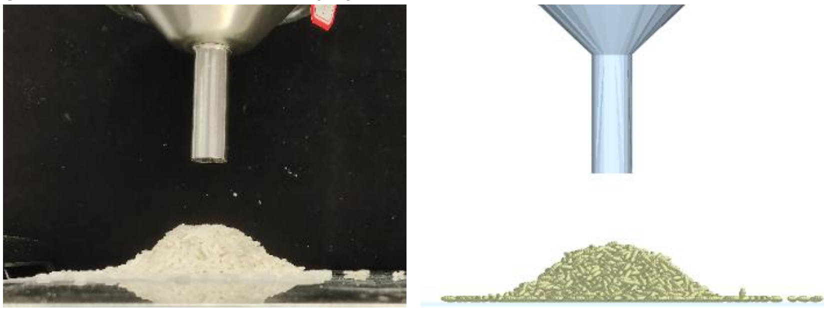

a) *b)*

Fig. 3 - Measurement of AOR
a) physical AOR; b) simulation AOR

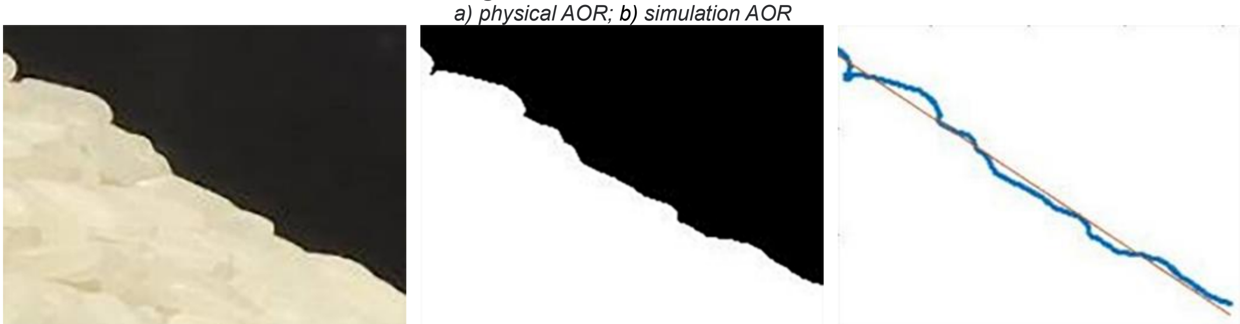

a) *b)* *c)*

Fig. 4 - Image processing
a) original image; b) binarization image; c) boundary fitting image

Intrinsic parameters of white rice

The Poisson's ratio, shear modulus and density intrinsic parameter ranges of white rice and stainless steel were determined through relevant literature (*Shitanda et al., 2002; Han et al., 2016; Zeng et al., 2017; Qiao et al., 2020*), as shown in Table 2.

Table 2

Material parameters obtained from literature

Parameters	Value	Source
White rice Poisson's ratio	0.2-0.3	(*Shitanda et al, 2002*)
Shear modulus of white rice/MPa	1-3.75	(*Han et al., 2016; Zeng et al., 2017*)
White rice density/(kg·m^{-3})	1350-1550	
Stainless steel Poisson's ratio	0.3	(*Qiao et al., 2020*)
Shear modulus of stainless steel/MPa	70000	
Stainless steel density/(kg·m^{-3})	7930	

Contact parameters of white rice

Restitution coefficient is a parameter to measure the deformation recovery ability of particles after collision. Free-fall test was used to measure the restitution coefficient. The test platform was shown in Fig. 5. With the coordinate paper as the test background, and the white rice fell stationary from 200 mm (H) each time and bounced after collision with the stainless steel. The maximum height (h) of the white rice bounced was recorded when the particle vertical upward trend. The test was repeated for 10 times, and the restitution coefficient was calculated by Equation (4). The range of particle-stainless steel restitution coefficient of HWR was 0.32 to 0.56. The range of particle-stainless steel restitution coefficient of DWR was 0.35 to 0.74.

$$e = \frac{v_2}{v_1} = \sqrt{\frac{2gh}{2gH}} = \sqrt{\frac{h}{H}} \tag{4}$$

where:

v_1 - The normal relative velocity of two objects before a collision;

v_2 - The normal relative velocity of two objects after a collision.

In this paper, white rice was arranged and pasted on the stainless steel plate as the contact bottom plate (*Li et al., 2022*) for the collision test. It was used to measure the restitution coefficient between white rice and white rice. The test method was the same as above. The range of particle-particle restitution coefficient of HWR was 0.28 to 0.54. The range of particle-particle restitution coefficient of DWR was 0.3 to 0.47.

Fig. 5 - Test platform for restitution coefficient

1-graph paper; 2-laptop; 3-stainless steel plate; 4-high-speed camera; 5-fill-in light

The inclined plane method was used to measure the particle-particle static friction coefficient and particle-stainless steel static friction coefficient. The test device was shown in Fig. 6. In order to prevent white rice from rolling, two grains were glued together. The angle of the stainless steel plate was changed by adjusting the height of the lifting platform. When the white rice began to slide, the angle of digital protractor was recorded. The static friction coefficient was calculated using the following Equation (5). Each group was repeated 20 times. The range of particle-particle static friction coefficient of HWR was 0.49 to 0.93, and the range of particle-stainless steel static friction coefficient was 0.38 to 0.54. The particle-particle static friction coefficient of DWR ranged from 0.47 to 0.83, and the particle-stainless steel static friction coefficient ranged from 0.35 to 0.55.

$$u_f = \tan\theta \tag{5}$$

where: u_f - static friction coefficient of white rice;

θ - the inclination angle.

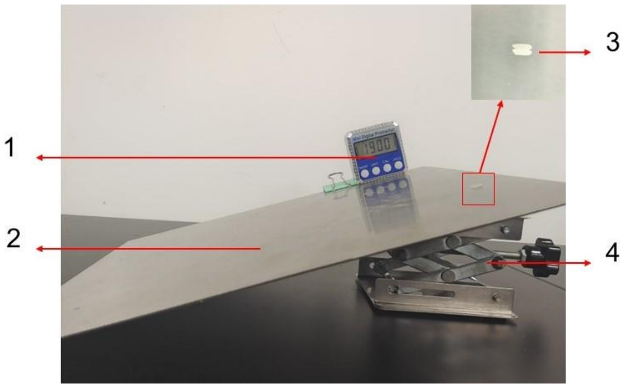

Fig. 6 - Test platform for static friction coefficient
1- digital protractor; 2- stainless steel plate; 3-whtie rice; 4- lifting platform

There is no standard method to measure the rolling friction coefficient at present. Through several simulation pre-tests and in combination with literature (*Han et al., 2014; Ma et al., 2022*), the range of particle-particle rolling friction coefficient is 0.001 to 0.15, and the range of particle-stainless steel rolling friction coefficient is 0.01 to 0.1.

RESULTS AND DISCUSSION

Analysis on the simulation results of PB test

In this study, the AOR of the physical test was used as the response value, and the PB test was designed by Minitab R20 (Pennsylvania State University, Commonwealth of Pennsylvania, USA). The parameters that significantly affected the AOR of HWR and DWR were screened out respectively. The 9 DEM parameters were represented by X_1~X_9, and each parameter was set at high (+1) and low (-1) levels. Each parameter range was determined based on the literature and the test and simulation pre-test in this paper. The same level values were used because the measurements of the two white rice varieties were not significantly different. The levels of PB test are shown in Table 3. The design and results of PB test are shown in Table 4. Table 4 shows that the AOR of white rice with different types are obviously different at the same parameters level, and the maximum difference in the AOR between two white rice varieties is 8.22°

Table 3

Factors and levels of PB test

Symbol	Parameters	Level	
		-1	+1
X_1	Poisson's ratio	0 .2	0.3
X_2	Density/kg·m^{-3}	1350	1550
X_3	Shear modulus/MPa	1	3.75
X_4	Particle-particle restitution coefficient	0.25	0.55
X_5	Particle-particle static friction coefficient	0.45	0.95
X_6	Particle-particle rolling friction coefficient	0.001	0.15
X_7	Particle-stainless steel restitution coefficient	0.3	0.6
X_8	Particle-stainless steel static friction coefficient	0.35	0.55
X_9	Particle-stainless steel rolling friction coefficient	0.01	0.1

Minitab R20 software was used to analyze the Significance of the PB test results. The analysis results of HWR and DWR are shown in Table 5. According to Table 5, the particle-particle static friction coefficient X_5 and particle-particle rolling friction coefficient X_6 have significant effects on the AOR of HWR and DWR. The remaining parameters have no significant effect on the AOR.

Table 4

Design and results of PB test

Number	X_1	X_2	X_3	X_4	X_5	X_6	X_7	X_8	X_9	HWR AOR β_i / (°)	DWR AOR β_j / (°)
1	1	-1	1	1	-1	-1	-1	-1	1	33.91	25.69
2	1	1	-1	1	1	-1	-1	-1	-1	32.31	28.58

Number	X_1	X_2	X_3	X_4	X_5	X_6	X_7	X_8	X_9	HWR AOR β_i / (°)	DWR AOR β_j / (°)
3	-1	1	1	-1	1	1	-1	-1	-1	50.25	45.58
4	-1	-1	1	1	-1	1	1	-1	-1	45.57	43.26
5	1	-1	-1	1	1	-1	1	1	-1	34.43	30.66
6	1	1	-1	-1	1	1	-1	1	1	50.27	46.90
7	1	1	1	-1	-1	1	1	-1	1	40.85	44.23
8	1	1	1	1	-1	-1	1	1	-1	30.99	28.72
9	-1	1	1	1	1	-1	-1	1	1	33.42	31.84
10	1	-1	1	1	1	1	-1	-1	1	51.75	44.21
11	-1	1	-1	1	1	1	1	-1	-1	49.30	45.70
12	1	-1	1	-1	1	1	1	1	-1	52.15	44.83
13	-1	1	-1	1	-1	1	1	1	1	42.69	41.56
14	-1	-1	1	-1	1	-1	1	1	1	36.05	31.94
15	-1	-1	-1	1	-1	1	-1	1	1	45.63	41.90
16	-1	-1	-1	-1	1	-1	1	-1	1	34.28	29.03
17	1	-1	-1	-1	-1	1	-1	1	-1	43.60	43.10
18	1	1	-1	-1	-1	-1	1	-1	1	32.75	28.42
19	-1	1	1	-1	-1	-1	-1	1	-1	31.02	29.57
20	-1	-1	-1	-1	-1	-1	-1	-1	-1	27.74	26.42

Table 5

Significance analysis of PB test for HWR and DWR

Parameters	Effect		Sum of squares		*P* value	
	HWR	DWR	HWR	DWR	HWR	DWR
X_1	0.706	-0.146	2.49	0.11	0.5184	0.7725
X_2	-1.126	1.006	6.34	5.06	0.3408	0.0678
X_3	1.296	0.760	8.40	2.89	0.2473	0.1530
X_4	0.104	-0.790	0.05	3.12	0.9234	0.1390
X_5	4.946	2.640	122.31	34.85	0.0009**	0.0003**
X_6	14.516	15.040	1053.57	1131.01	<0.0001**	<0.0001**
X_7	-0.084	0.456	0.04	1.04	0.9381	0.3753
X_8	0.154	0.990	0.12	4.90	0.8868	0.0716
X_9	0.424	-0.070	0.9	0.02	0.6962	0.8895

*Note: ** indicates highly significant (P<0.01), and * indicates significant (P<0.05), the same below.*

Analysis on the simulation results of steepest ascent test

Based on the results of PB test, significance parameters (X_5 and X_6) were selected for the steepest ascent test. The Particle-particle static friction coefficient was taken as 0.45-0.7. The Particle-particle rolling friction coefficient was taken as 0-0.075, and the remaining parameters were based on the average values in Table 3. The steepest ascent test design and results for HWR and DWR are shown in Table 6, respectively. The relative error (Y) between the AOR of simulation test (β) and the AOR of physical test (α) was calculated by Equation (6). When the relative error of AOR was the smallest, the adjacent steepest ascent test level was selected as the central composite optimization test parameter range.

$$Y = \frac{|\beta - \alpha|}{\alpha} \tag{6}$$

As shown in Table 6, the relative errors of the AOR of the steepest ascent test and the physical test decreased first and then increased. The relative errors of the AOR of the HWR steepest ascent test number 2 was the smallest, and the DWR steepest ascent test number 3 was the smallest. Therefore, the steepest ascent test number 1 and number 3 of HWR were selected as low (-1) level and high (+1) level respectively for the subsequent central composite test design. Number 2 and number 4 of DWR were selected as low (-1) level and high (+1) level respectively for the subsequent central composite test design.

Table 6

Design and results of steepest ascent test of HWR and DWR

Number	X_5	X_6	Simulation AOR / °		Relative error / %	
			HWR / β_i	DWR / β_j	HWR/ Y_i	DWR/ Y_j
1	0.45	0	30.15	28.98	6.89	13.39
2	0.5	0.015	32.94	31.20	1.73	6.75
3	0.55	0.03	36.22	34.01	11.86	1.64
4	0.6	0.045	38.72	35.18	19.57	5.14
5	0.65	0.06	42.06	38.14	29.89	13.99
6	0.7	0.075	42.65	39.79	31.72	18.92

Analysis on the simulation results of central composite test

The central composite test was used to seek the optimal parameter combination of significance parameters such as particle-particle static friction coefficient and particle-particle rolling friction coefficient in the simulation test. The factor level ranges of particle-particle static friction coefficient and particle-particle rolling friction coefficient were obtained according to the steepest ascent test, and the factor levels of the central composite test are shown in Table 7. Design of central composite test was carried out by using Minitab R20 software. The design and results of central composite test are shown in Table 8. The mean values in Table 3 were used for the remaining parameters of the central composite test.

Table 7

Factors and levels of central composite test

Factor	level			
	-1		1	
	HWR	DWR	HWR	DWR
X_5	0.45	0.5	0.55	0.6
X_6	0	0.015	0.03	0.045

The regression models of AOR with particle-particle static friction coefficient (X_5) and particle-particle rolling friction coefficient (X_6) were established by binary regression fitting on the results of the central composite test. The regression equation of HWR is shown in Equation (7), and the regression equation of DWR is shown in Equation (8).

$$\beta_i = 33.446 + 0.722 X_{5i} + 2.549 X_{6i} - 1.794 X_{5i}^2 - 1.686 X_{6i}^2 + 0.062 X_{5i} X_{6i} \quad (7)$$

$$\beta_j = 34.327 + 0.43 X_{5j} + 2.511 X_{6j} + 2.133 X_{5j}^2 - 2.007 X_{6j}^2 + 0.157 X_{5j} X_{6j} \quad (8)$$

ANOVA was performed on the results of central composite test for HWR and DWR, and the results were shown in Table 8. The regression model of AOR of HWR and DWR are P<0.0001, and the P value of the lack of fit is greater than 0.05, indicating that the two models are extremely significant, and the lack of fit is not significant. The determination coefficient R^2 is 0.9753 and 0.9671 respectively, indicating that the two regression equations fit well and were reliable. The effect of X_{5i}, X_{6i}, X_{5i}^2 and X_{6i}^2 on the AOR of HWR and DWR was significant, while the effect of $X_{5i}X_{6i}$ on the AOR was not significant.

Table 8

Design and results of central composite test

Number	X_5	X_6	HWR AOR β_i / (°)	DWR AOR β_j / (°)
1	-1	-1	30.06	31.77
2	+1	-1	31.73	32.30
3	-1	+1	35.11	36.31
4	+1	+1	36.53	37.49
5	-0.5	0	32.69	34.49
6	+0.5	0	33.01	34.90

Number	X_5	X_6	HWR AOR β_i / (°)	DWR AOR β_j / (°)
7	0	-0.5	32.10	32.07
8	0	+0.5	35.34	35.25
9	0	0	33.60	34.87
10	0	0	33.61	34.11
11	0	0	33.36	33.96
12	0	0	33.22	34.70
13	0	0	33.96	34.55

Table 9

ANOVA of HWR and DWR for central composite test

Source	Degree of freedom	Sum of squares		Mean square		*P* value	
		HWR	DWR	HWR	*DWR*	*HWR*	*DWR*
Model	5	32.38	30.42	6.48	6.08	<0.0001**	<0.0001**
X_{5i}	1	2.35	0.83	2.34	0.83	0.0029**	0.0494*
X_{6i}	1	29.24	28.38	29.24	28.38	<0.0001**	<0.0001**
$X_{5i}X_{6i}$	1	0.02	0.10	0.02	0.10	0.7260	0.4396
X_{5i}^2	1	0.78	1.11	0.78	1.11	0.0362**	0.0289*
X_{6i}^2	1	0.69	0.98	0.69	0.98	0.0453**	0.0366*
Residual	7	0.82	1.03	0.12	0.15		
Lack of fit	3	0.50	0.43	0.16	0.14	0.2432	0.4990
Pure error	4	0.32	0.61	0.07	0.15		
Sum	12	33.21	31.45				

Verification test

Using the optimization design in Minitab R20 software, the AOR of HWR physical test 32.38° and the AOR of DWR physical test 33.46° were taken as the target values to substitute into their respective regression models for solution. The optimal combination of the significance parameters of HWR: the particle-particle static friction coefficient was 0.5 and particle-particle rolling friction coefficient was 0.0146. The optimal combination of significance parameters of DWR: the particle-particle static friction coefficient was 0.55 and particle-particle rolling friction coefficient was 0.0258. Other non-significant simulation parameters were averaged from Table 3. The DEM test was verified under the condition of optimal parameter combination, each group of tests was repeated 3 times. The comparison between simulated AOR and physical AOR is shown in Fig. 7. The AOR of HWR simulation test are 32.64°, 34.02° and 33.27°, respectively, and the relative error of AOR are 2.42%, 1.67% and 0.57%. The AOR of DWR simulation test are 33.29°, 32.70° and 33.36°, respectively, and the relative error of AOR are 0.51%, 2.25% and 0.29%. The relative error of the DEM test and physical test of the two varieties of white rice is less than 3%. The results of AOR test show that the DEM test have high similarity to the physical test, which indicates that the DEM parameters of HWR and DWR are accurate and reliable.

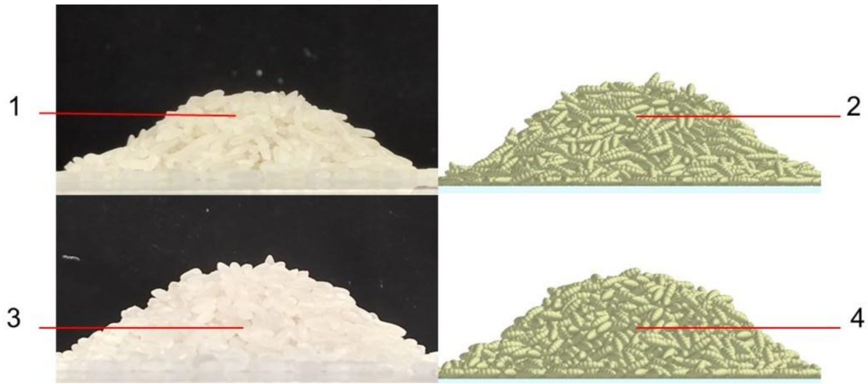

Fig. 7 - Comparison of AOR test of white rice

1-physical test of HWR; 2-simulation test of HWR; 3-physical test of DWR; 4-simulation test of DWR

CONCLUSIONS

In this paper, Huanghuazhan, an indica rice, and Dongnong 429, a japonica rice, were selected as the research objects. The DEM was used to calibrate white rice DEM parameters, and the accuracy and reliability of DEM parameter calibration were verified by physical AOR test. The conclusions are as follows:

(1) The triaxial dimensions of HWR and DWR were determined. Two kinds of discrete element models of HWR and DWR were established by multi-ball filling method. The DEM significance parameters and their optimal intervals of HWR and DWR were determined by PB test and steepest ascent test, respectively. The optimal range of significance parameters for HWR was as follows: the range of particle-particle static friction coefficient was 0.45 to 0.55, the range of particle-particle rolling friction coefficient was 0 to 0.015. The optimal range of significance parameters for DWR was as follows: particle-particle static friction coefficient was 0.5 to 0.6, particle-particle rolling friction coefficient was 0.015 to 0.045. Regression models of AOR and simulation parameters of HWR and DWR were established by central composite test. The coefficient of determination of HWR regression model and DWR regression model were 0.9753 and 0.9671 respectively.

(2) The AOR of physical test of HWR and DWR were taken as the target value to substitute into their respective regression models for solution. The optimal combination of significance parameters of HWR: the particle-particle static friction coefficient was 0.5 and the particle-particle rolling friction coefficient was 0.0146. The optimal combination of significant parameters of DWR: the particle-particle static friction coefficient was 0.55 and the particle-particle rolling friction coefficient was 0.0258. The relative error of the DEM test and physical test of the two varieties of white rice is less than 3%. The similarity of pile shape of HWR and DWR in simulation and physical test is high, which indicates that the DEM parameters are reliable. This calibration method can be used for discrete element calibration of related grains. It provides reference for the subsequent study on the adaptability of different varieties of machinery.

ACKNOWLEDGMENTS

The authors express their acknowledgment to the National Natural Science Foundation of China (Grant No. 32001423) and Natural Science Foundation of Hubei Province (Grant No. 2020CFB471) for financial support and all of the persons who assisted in this writing.

REFERENCES

[1] Ahmed, S.B., Ali, S.F., Khan, A.Z. (2021). On the frontiers of rice grain analysis, classification and quality grading: A review. *IEEE Access*, 9, 160779-160796. https://doi.org/10.1109/access.2021.3130472

[2] Gong, X., Bai, X., Huang, H., Zhang, F., Gong, Y., Wei, D. (2021). DEM parameters calibration of mixed biomass sawdust model with multi-response indicators. *INMATEH-Agricultural Engineering*, 65(3), 183-192. https://doi.org/10.35633/inmateh-65-19

[3] Han, Y., Jia, F., Tang, Y., Liu, Y., Zhang, Q. (2014). Influence of granular coefficient of rolling friction on accumulation characteristics (颗粒滚动摩擦系数对堆积特性的影响). *Acta Physica Sinica,* 63(17), 173-179. https://doi.org/10.7498/aps.63.174501

[4] Han, Y., Jia, F., Zeng, Y., Jiang, L., Zhang, Y., Cao, B. (2016). Effects of rotation speed and outlet opening on particle flow in a vertical rice mill. *Powder Technology*, 297, 153-164. https://doi.org/10.1016/j.powtec.2016.04.022

[5] Li, H., Zeng, R., Niu, Z., Zhang, J. (2022). A calibration method for contact parameters of maize kernels based on the discrete element method. *Agriculture*, 12(5), 664. https://doi.org/10.3390/agriculture12050664

[6] Liu, F., Li, D., Zhang, T., Lin, Z., Zhao, M. (2020). Analysis and calibration of quinoa grain parameters used in a discrete element method based on the repose angle of the particle heap. *INMATEH-Agricultural Engineering*, 61(2), 77-86. https://doi.org/10.35633/inmateh-61-09

[7] Liu, W., He, J., Li, H., Li, X., Zheng, K., Wei, Z. (2018). Calibration of Simulation Parameters for Potato Minituber Based on EDEM (基于离散元的微型马铃薯仿真参数标定). *Transactions of the Chinese Society for Agricultural Machinery,* 49(5), 12. https://doi.org/10.6041/j.issn.1000-1298.2018.05.014

[8] Lu, L., Fang, C., Hu, Z., Hu, X., Zhu, Z. (2019). Grade classification model tandem BpNN method with multi-metal sensor for rice eating quality evaluation. *Sensors and Actuators B: Chemical*, 281, 22-27. https://doi.org/10.1016/j.snb.2018.10.062

[9] Ma, Z., Traore, S. N., Zhu, Y., Li, Y., Xu, L., Lu, E., Li, Y. (2022). DEM simulations and experiments investigating of grain tank discharge of a rice combine harvester. *Computers and Electronics in Agriculture*, 198, 107060. https://doi.org/10.1016/j.compag.2022.107060

[10] Markauskas, D., Kačianauskas, R. (2011). Investigation of rice grain flow by multi-sphere particle model with rolling resistance. *Granular Matter*, 13, 143-148. https://doi.org/10.1007/s10035-010-0196-5

[11] Qiao, X., Jia, H., Wang, C., Wang, K., Yan, B., Guo, W. (2020). Design and experiment of ozone sterilizer device for organic matrix (有机基质臭氧消毒设备设计与试验). *Transactions of the Chinese Society for Agricultural Machinery*, 51(07), 138-145. https://doi.org/10.6041/j.issn.1000-1298.2020.07.016

[12] Riaz, M., Ismail, T., Akhtar, S. (2017). Harvesting, threshing, processing, and products of rice. *Rice Production Worldwide*, 419-453. https://doi.org/10.1007/978-3-319-47516-5_16

[13] Shitanda, D., Nishiyama, Y., Koide, S. (2002). Compressive strength properties of rough rice considering variation of contact area. *Journal of Food Engineering*, 53(1), 53-58. https://doi.org/10.1016/s0260-8774(01)00139-x

[14] Zeng, Y., Jia, F., Zhang, Y., Meng, X., Han, Y., Wang, H. (2017). DEM study to determine the relationship between particle velocity fluctuations and contact force disappearance. *Powder Technology*, 313, 112-121. https://doi.org/10.1016/j.powtec.2017.03.022

[15] Zeng, Z., Ma, X., Cao, X., Li, Z., Wang, Xi. (2021). Critical Review of Applications of Discrete Element Method in Agricultural Engineering (离散元法在农业工程研究中的应用现状和展望). *Transactions of the Chinese Society for Agricultural Machin*ery, 52(4), 1-20. https://doi.org/10.6041/j.issn.1000-1298.2021.04.001

[16] Zhao, H., Huang, Y., Liu, Z., Liu, W., Zheng, Z. (2021). Applications of discrete element method in the research of agricultural machinery: A review. *Agriculture*, 11(5), 425. https://doi.org/10.3390/agriculture11050425

[17] Zhao, L., Duan, X., Liu, H. (2023). Novel Grade Classification Tool with Lipidomics for Indica Rice Eating Quality Evaluation. *Foods*, 12(5), 944. https://doi.org/10.3390/foods12050944